Journal of Energy and Power Engineering 18 (2024) 1-8
doi: 10.17265/1934-8975/2024.01.001

Simulation and Performance Analysis of Six Types of Sun Tracker Approaches: A Comparative Analysis for Solar Concentrating Technology Application at Burkina Faso

Stanislas Sanfo[1, 3], Serge Dimitri Bazyomo[2], Tizane Daho[1] and Abdoulaye Ouedraogo[1]

1. Laboratoire de Physique et de Chimie de l'Environnement (LPCE), Departement de Physique, Unité de Formation et de Recherche en Sciences Exactes et Appliquées, Université Joseph KI-ZERBO, Ouagadougou, BP 7021, Burkina Faso

2. Laboratory of Thermal and Renewable Energies Department of Physics, Unit of Training and Research on Exact and Applied Sciences, University Joseph KI-ZERBO, Ouagadougou, BP 7021, Burkina Faso

3. Laboratoire Recherche Développement (LARED), Université de Ouahigouya, Burkina Faso

Abstract: Modelization equations of six approaches for tracking the sun are recalled and used to evaluate the constraints and performances to which they lead to. The geographical study case is taken for the specific latitude of 12 North that is a good matching with the location of the country of Burkina Faso. Three decisive periods were locally established in order to consider the different travels of the sun on sky during one year. This work presents some technical data which facilitates the choice of sun tracking approaches with concern of a concentrator limits such as its angle of acceptance, its motion control card interpolation model, or its minimum irradiation level for energy conversion effectiveness.

Key words: Solar radiation, sun tracker, Burkina Faso, experimental data.

Nomenclature

α: Collector aperture orientation angle

β: Collector aperture inclination angle

δ_S: Sun declination according to earth equator

θ_I: Incidence angle

θ_L: Longitudinal angle of incidence

θ_T: Transversal angle of incidence

$\theta_{\max}$: Acceptance angle

ϕ: Geographical latitude

ψ: Solar constant

ϖ: Hour angle

a: Azimuth angle

f_{atm} : Direct sun rays transmitivity factor or attenuation factor

h: Elevation angle

$\vec{n}$: Normal to the collector aperture

z: Zenithal distance

$\psi_{\text{th,gl0}}$: Theoretical instantaneous irradiation

N_{jr}: Day number in the calendar from 1 to 365

$\vec{u}$: Unit vector carrying the direction of the sun

1. Introduction

The sun-tracking system plays an important role in the development of solar energy applications, especially for the high solar concentration systems that directly convert solar energy into thermal or electrical energy [1]. For sun tracking systems, the difficulties are to manufacture the tracker mechanism, to encode the algorithm and reduce the energy supply used for following the sun.

Corresponding author: Stanislas Sanfo, Dr, maître assistant, research fields: mechanical and energy.

Another point is the dynamic range of motion for a practical sun tracker that is about ±70 ° and ±140 ° for elevation and azimuth directions, respectively.

Whatever the type of sun tracker, the kinetic implications and the energy performances vary according to the concentrator's optical properties, the date, the time and the geographical information. In order to maintain high output power and stability of the solar power system, an appropriate sun-tracking system must be chosen in close relation to the specific characteristics; generally the higher the system acceptance angle the more possibilities of choice we have for the sun tracker and the period of radiation collection. So, in this section, we study constraints related to the adoption of a type of sun tracker, on a given geographical zone, according to the hour. The present study will be undertaken for the latitude of 12 ° North which particularly takes into account the country of Burkina Faso, and will concern three established periods in the year. We address the questions of motion fulfillment, the range of concentrator acceptance angle, both in longitudinal and transversal direction and the rate of energy at the collector aperture.

The importance to conduct this study is the fact that there is a lack of technical data sheets about the constraints and performances leads by the adoption of sun-tracking approaches according to the date, the time and the region on earth. Thanks to this study, industrials and solar central companies can find data to make the choice of convenient sun tracker in the country.

2. Methodology

Comparisons are done for three sun tracking mechanisms (no tracker, one-axis sun tracker and two-axis sun tracker). For each mechanism there can be one to three types of sun tracker processes [2]. Our study cases are:

- **Track1**: a two-axis sun tracker, the tracking axis operates in azimuth and elevation senses.
- **Track2**: a no tracker, a fixed tilt is applied to the system (i.e. latitude-tilted-axis in North-South direction) here a tilt of 12 °South.
- **Track3**: a one-axis sun tracker, the tracking axis is tilted from the horizon by an angle oriented along North-South direction so that the normal surface is aligned with the sun each noon.
- **Track4**: a one-axis sun tracker, the tracking axis is to remain parallel to the surface of the earth and it is always oriented along North-South direction; the tracking is operated from East to West.
- **Track5**: a one-axis sun tracker, the tracking axis is to remain parallel to the surface of the earth and it is always oriented along East-West direction; the tracking is operated from North to South.
- **Track6**: a two-axis sun tracker, the tracking axis is to remain parallel to polar axis and the tracking is operated from North to South.

In the present work we consider the general formula for on-axis sun tracking system without the transformation from earth-center frame to earth-surface frame. Referring to the literatures [3-10], the sun's azimuth and elevation angles can be determined by the sun position formula or algorithm at the given date, time and geographical information:

$$\delta_s = 23.45 \sin\left[\frac{360}{365}\left(284 + N_{jr}\right)\right] \quad (1)$$

$$\omega = (TVS - 12) \times 15 \quad (2)$$

$$h = \frac{\pi}{2} - z = \sin^{-1}[\sin\emptyset \sin\delta_s + \cos\emptyset \cos\delta_s \cos\omega] \quad (3)$$

$$\alpha = \begin{cases} \alpha_{so} \text{ if } \cos\omega \geq \tan\delta_s / \tan\phi \\ \text{else} \begin{cases} 0 \text{ if } \omega = 0 \\ -\pi + |\alpha_{so}| \text{ if } \omega < 0 \\ \pi - \alpha_{so} \text{ if } \omega > 0 \end{cases} \end{cases}$$

with

$$\sin\alpha_{so} = \frac{\cos\delta_s \sin\omega}{\cos h}$$

At a given day, hour and altitude, the unit vector, $\vec{\mu}$, carrying the direction of the sun is given by:

$$\vec{\mu} = \begin{pmatrix} \cos h \sin\alpha \\ \cos h \cos\alpha \\ \sin h \end{pmatrix}$$

For each type of sun tracker process the solar collector is positioned at pre-calculated angles α and β which

are obtained from a special formula or algorithm found in literature [10-12]. They are registered in Table 1 with their involving incidence angle: We consider three appropriate periods for working out the functioning: the day of summer solstice (N_{jr} = 172), the day of winter solstice (N_{jr} = 355) and one of the two days for which the motion of the sun passes through the local zenith at noon (i.e. we considered the days when $\phi - \delta_s = 0$). Among the two days identified, N_{jr} = 112 and N_{jr} = 233, we make the arbitrary choice of the day (N_{jr} = 112) that we called local Equinox. For a given type of sun tracker, the theorical irradiation is approximated by Bernard [13, 14], and Daguenet [15]:

$$\psi_{\mathrm{th,gl0}} = \psi_0 \left[1 + 0.033 \cos\left(\frac{360}{365} N_{jr}\right)\right] \times \mathrm{f_{atm}} \cos\theta_{\mathrm{I}} \quad (4)$$

with

$$\mathrm{f_{atm}} = \mathrm{Aexp}(-\mathrm{B} \times \mathrm{m_h}) \text{ and } \mathrm{m_h} = \frac{\mathrm{p_{atm}}}{1000 \sin \mathrm{h}}$$

In line with M. Daguenet [15], we consider a clear sky, while taking A = 0.87 and B = 0.17 as constants for determining the atmospheric attenuation of irradiation f_{atm}. The insolation is approximated by triangular integration of $\psi_{th,gl0}$ with a step of 36 s, over duration of the daily insolation.

Fig. 1 describes the transversal angle of incidence and longitudinal angle of incidence, defined as the angle between incident sun rays and the transversal plane of the collector aperture, respectively the angle between incident sun rays and the longitudinal plane of the collector aperture.

The data from these two angles make it possible to appreciate the good alignment of the collector on the trajectory of the sun. To establish these angles, We proceed by projection of the unit vector, $\vec{\mu}$, on each plane. In fact, for a given collector positioned at pre-calculated sun-tracking angles α and β, the normal vector, $\vec{n}$, to its aperture is given:

$$\vec{n} = \begin{pmatrix} \cos\beta \sin\alpha \\ \cos\beta \cos\alpha \\ \sin\beta \end{pmatrix}$$

Let $\overrightarrow{W}$ be the projection of $\vec{\mu}$ in the transversal plane P_T of normal $\overrightarrow{n_L}$. This projection can be found by this calculation:

$$\overrightarrow{W} = \vec{n}_l \wedge (\vec{u} \wedge \vec{n}_L) \quad (5)$$

where

$$\vec{n}_L = \begin{pmatrix} \cos\alpha \\ -\sin\alpha \\ 0 \end{pmatrix} \quad (6)$$

Table 1 Formula for different sun tracking methods.

	Inclination	Orientation	Incidence angle
Track1	$\beta = z$	$\alpha = \alpha$	$\cos\theta_1 = 1$
Track2	$\beta = \phi$	$\alpha = 0$	$\cos\theta_1 = \sin(\phi \pm \beta)\sin\delta_s + \cos(\phi \pm \beta)\cos\delta_s \cos\varpi$
Track3	$\beta = \phi - \delta_s$	$\alpha = 0$	$\cos\theta_1 = \sin^2\delta_s + \cos^2\delta_s \cos\omega$*
Track4	$\tan\beta = \tan z \lvert\cos(\alpha - \alpha)\rvert$	$\alpha = \begin{cases} 90\ if\ a \succ 0 \\ -90\ otherwise \end{cases}$	$\cos\theta_1 = (\sin^2 h = \cos^2\delta \sin^2\omega)$**
Track5	$\tan\beta = \tan z \lvert\cos(\alpha)\rvert$	$\alpha = \begin{cases} 0\ if\ \lvert a\rvert \leqslant 90 \\ 180\ if\ \lvert a\rvert \succ 90 \end{cases}$	$\cos\theta_1 = (1 - \cos^2\delta \sin^2\varpi)$
Track6	$\tan\beta = \tan\emptyset / \cos\alpha$	$\alpha = \tan^{-1}\left(\frac{\sin z \sin a}{\cos\theta_1 \sin\phi}\right) + 180 C_1 C_2$ $C_1 = \begin{cases} 1\ if\ \left(\tan^{-1}\left(\frac{\sin z \sin a}{\cos\theta_1 \sin\phi}\right)\ a \geqslant 0\right) \\ 0\ otherwise \end{cases}$ $C_2 = \begin{cases} 1\ if\ a \geqslant 0 \\ -1\ otherwise \end{cases}$	$\cos\theta_1 = \cos z \cos\phi + \sin z \sin\phi \cos a$

* from Refs. [10, 12].

** from Refs. [11, 10].

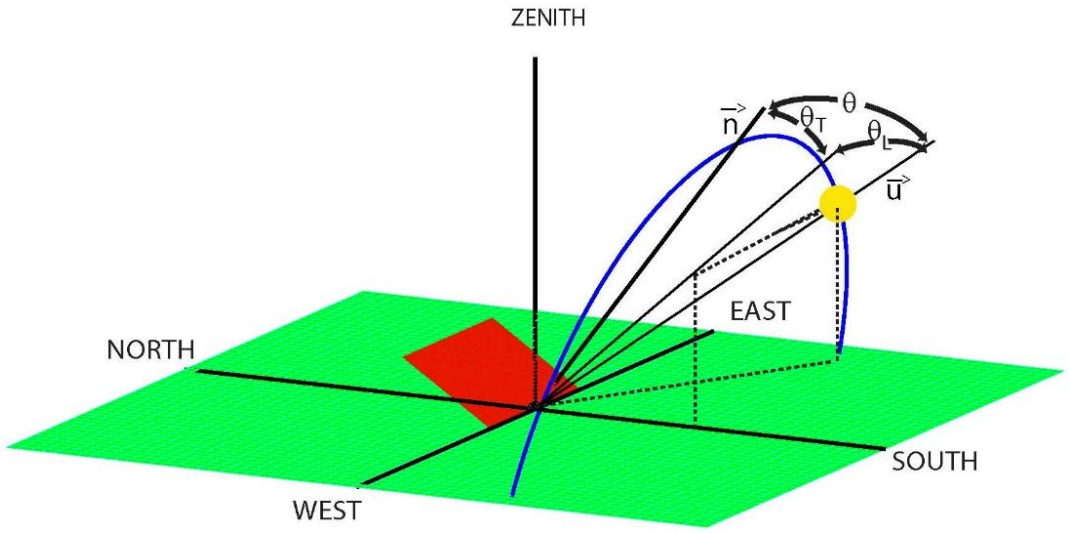

Fig. 1 Transversal and longitudinal incidence angles at the collector aperture.

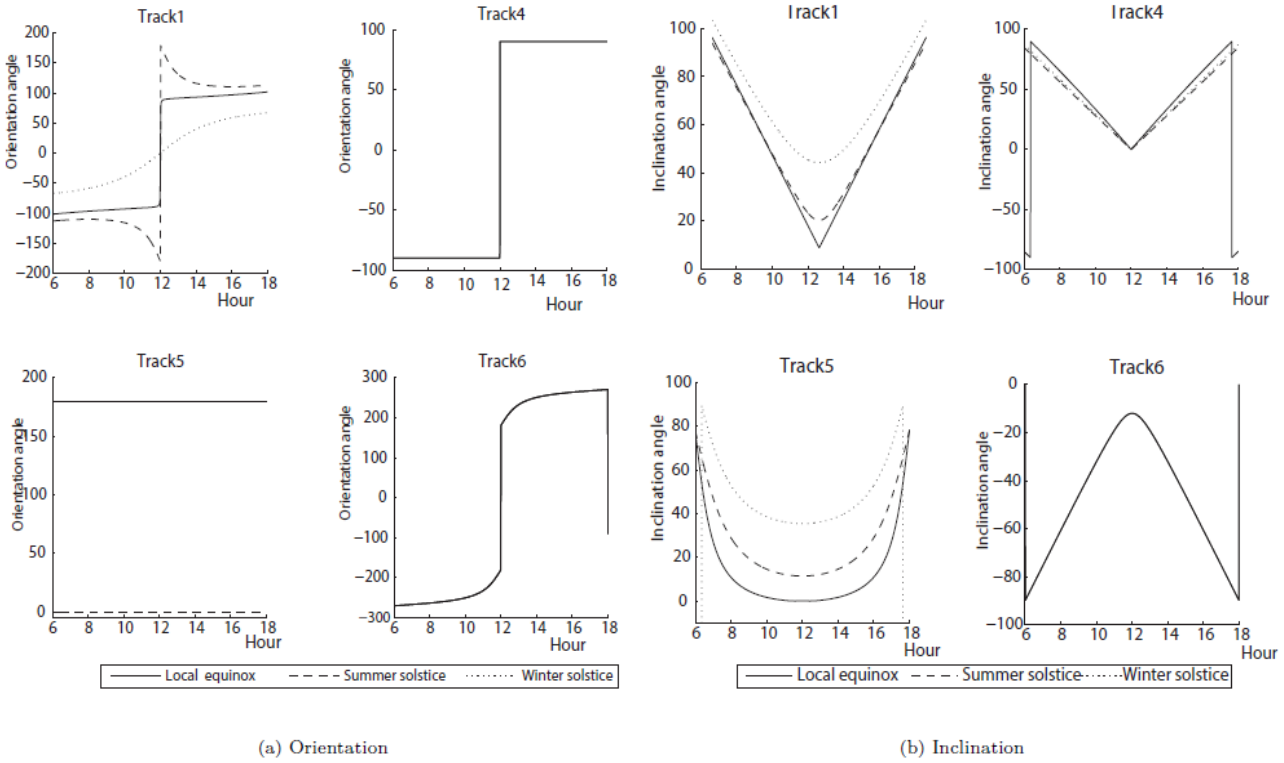

(a) Orientation (b) Inclination

Fig. 2 Angular motion (a) orientation, and (b) inclination, to be applied according to the type of sun tracker, to the three chosen periods and the hour.

So the longitudinal angle of incidence, θ_L, and the transversal angle of incidence, θ_T, are calculated as follow:

$$\theta_L = \cos^{-1}\left(\frac{\vec{\mu}\cdot\vec{W}}{\|\vec{\mu}\|\|\vec{W}\|}\right) \quad (7)$$

$$\theta_T = \cos^{-1}\left(\frac{\vec{n}\cdot\vec{W}}{\|\vec{n}\|\|\vec{W}\|}\right) \quad (8)$$

3. Results

3.1 Comparison of Different Types of Sun Tracker according to Kinematic Motion

Our interest in this study is to find out similarity between hourly angular motions for a given type of sun tracker, whatever the period of the year. Such a result

lets us foresee an easy manufacture of sun tracking mechanism. Generally, the motions are integrated as an algorithm into a microprocessor- or computer-based controller.

Figs. 2a and 2b show the needed angular motion to apply according to the hour and the period for one-axis sun tracking, and two-axis sun tracking. Through the analysis of layout curves obtained for the case of two-axis sun tracking, one can foresee that the automation of **Track1** requires completely different algorithms per day. On the other hand, for **Track6**, the regular and super-imposable curves obtained show that the same algorithm is enough for all the days of the year.

For one-axis sun tracker, the layout of curves suggests a changing algorithm per day. However, for the case of **Track4**, the layout of curves is linear and almost the same, so the choice of basic algorithm with a slight parametric adjustment can be made. Conversely, the layouts of curves of **Track5** are neither linear nor super-imposable; this can be a case of complex algorithm. So that, **Track4** and **Track6** seem to be the sun tracker mechanisms the easiest to implement at 12 °North.

3.2 Comparison of Sun Tracker Types on the Basis of Acceptance Angle to Be Reached for the Concentrator

Fig 3 shows the acceptance angles in longitudinal and transversal direction according to the period and to the hour. In Fig. 3a the layouts show some open parabolic curves with their maximum around 90 °reached at 6:00 or 18:00, and with their minimum reached at noon, around 0 ° for **Track3** & around different value 0 °, 11.45 ° or 35.45 ° for **Track2**. On the contrary symmetric curves are obtained for **Track6**, with minimum around 2.51 ° or 5.15 ° reached at 6:00 or 18:00 and maximum around 11.92 °or 23.45 °reached at noon. With **Track1**, **Track4** & **Track5** some layouts made of lines which are close to 0 ° are obtained for 6:00 or 18:00.

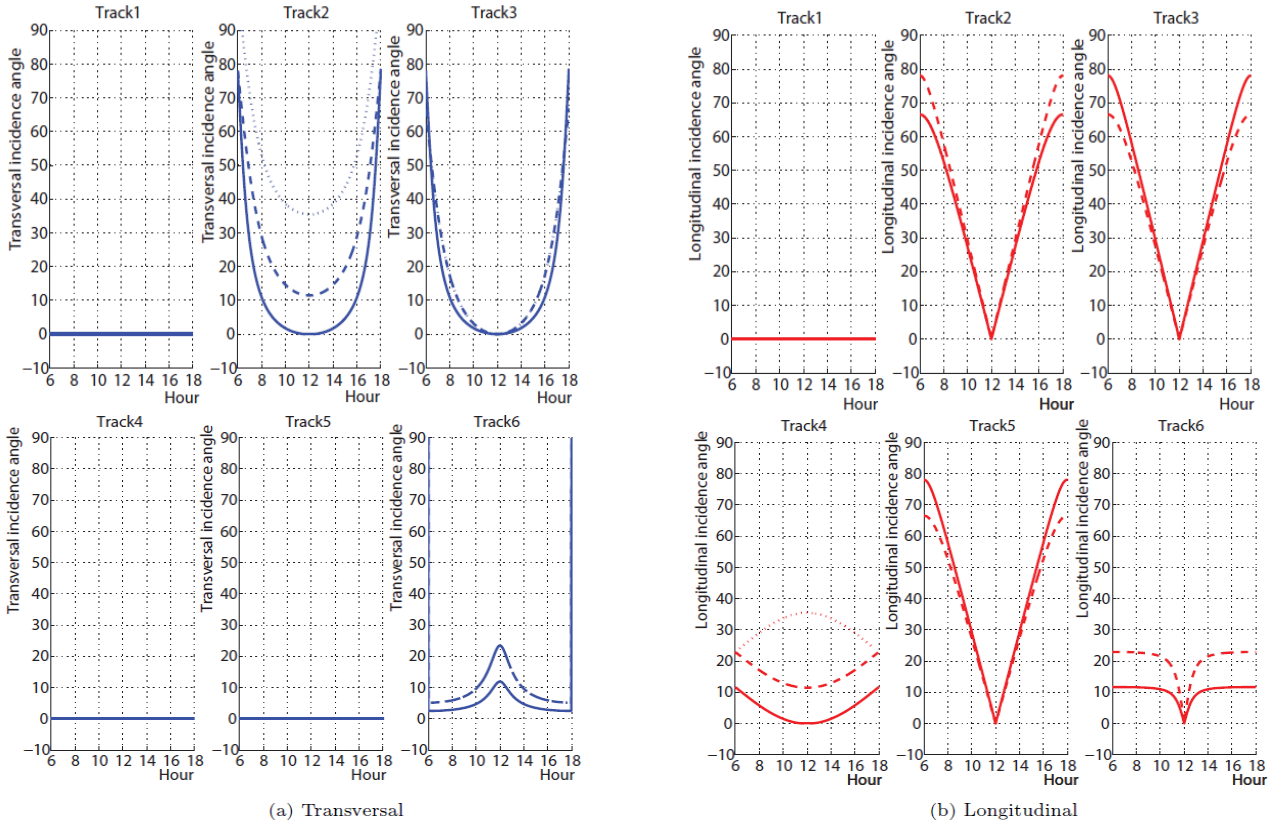

(a) Transversal (b) Longitudinal

Fig. 3 Evolution of (a) transversal and (b) longitudinal incidence angle according to the type of sun tracker, the three chosen periods and the hour.

Table 2 Range of extrema incidence angle in transversal and longitudinal direction.

Incidence plane	Type of sun tracker	Extrema incidence angle from 6:00 to 18:00		
		N_{jr} 112	Nj_r 172	Njr 355
Transversal	**Track1**	≈0 °	≈0 °	≈0 °
	Track2	0 °-90 °	11.45 °-90 °	35.45 °-90 °
	Track3	0 °-90.07 °	0 °-78.55 °	0 °-54.55 °
	Track4	≈0 °	≈0 °	≈0 °
	Track5	≈0 °	≈0 °	≈0 °
	Track6	2.51 °-11.92 °	5.15 °-23.45 °	5.17 °-23.45 °
Longitudinal	**Track1**	≈0 °	≈0 °	≈0 °
	Track2	0 °-78.07 °	0 °-66.55 °	0 °-65.99 °
	Track3	0 °-78.07 °	0 °-66.55 °	0 °-65.99 °
	Track4	0 °-12.19 °	11.44 °-24.00 °	24.00 °-35.44 °
	Track5	0 °-78.07 °	0 °-66.55 °	0 °-65.99 °
	Track6	0 °-11.66 °	0 °-22.99 °	0 °-22.90 °

In Fig. 3b the layouts obtained show curves near V shape with maximum around 66.55 ° or 78.07 ° reached at 6:00 or 18:00, and minimum close to 0 ° at noon for **Track2**, **Track3** & **Track5**. On the contrary layouts made of lines which are close to 0 ° are obtained for 6:00 or 18:00 with **Track1**. Symmetric curves with maximum around 11.66 ° or 23 ° reached at 6:00 or 18:00 and minimum close to 0 ° at noon are obtained with **Track6**. **Track4** gives parabolic opened layouts in summer solstice and local equinox with maximum around 12.19 ° or 24 ° reached at 6:00 or 18:00 and minimum respectively around 0 ° or 11.44 °, while a closed parabolic curve is obtained during winter solstice with minimum around 24 ° reached at 6:00 or 18:00 and maximum around 35.44 ° at noon.

Table 2 is a statement of extreme angle of acceptance to be reach in other to collect sun rays from 6:00 or 18:00 during the year, based on Fig. 3.

Over the year, we can interpret that only **Track1**, **Track4** & **Track5** lead to transversal angles of incidence always close to 0 °. The values of θ_T is laid between a relatively smooth gap from 2.51 ° to 23.45 ° for the case of **Track6** and is between a great gap from 0 ° to 90 ° for **Track2** and **Track3**. The longitudinal angle of incidence is close to 0 ° only for **Track1**. One records values ranging from 0 ° to 22.90 ° and 0 ° to 35.44 ° respectively for **Track6** and **Track4**. One records great gap going until 78 °, for **Track2**, **Track3** & **Track5**.

Considering the cosine factor, the maximum angle of acceptance to collect at least 90% of energy compared to normal incidence is approximately 25.84 °. **Track2** and **Track3** are far from being appropriate for high performance of concentrating system from 6:00 or 18:00. With regard to two-axis sun tracker, it is noted that **Track5** is not very suitable, despite a transversal incidence angle close to 0 °, it records great longitudinal incidence angle near 78 °. On the other hand, **Track4** is more or less suitable except during the winter solstice when it is necessary to take up the challenge of a 35.44 ° longitudinal angle of acceptance. **Track1**, quite naturally makes it possible to consider systems with the very weak angles of acceptance. **Track6** can be considered, with a system whose transversal angle of acceptance reaches 23.45 ° at least and the longitudinal angle of acceptance reaches 22.9 ° at least.

3.3 Comparison of Different Types of Sun Tracker on the Capacity of Collecting Energy at the Aperture

Fig. 4 gives the evolution of irradiation according to the hour. During local solstice and summer solstice, the production seems to have the same layouts. The difference appears on the beginning of solar energy collection at sunrise and it ends at sunset, in such a way that a less rate of energy is obtained during the winter solstice particularly for **Track2** and **Track4**.

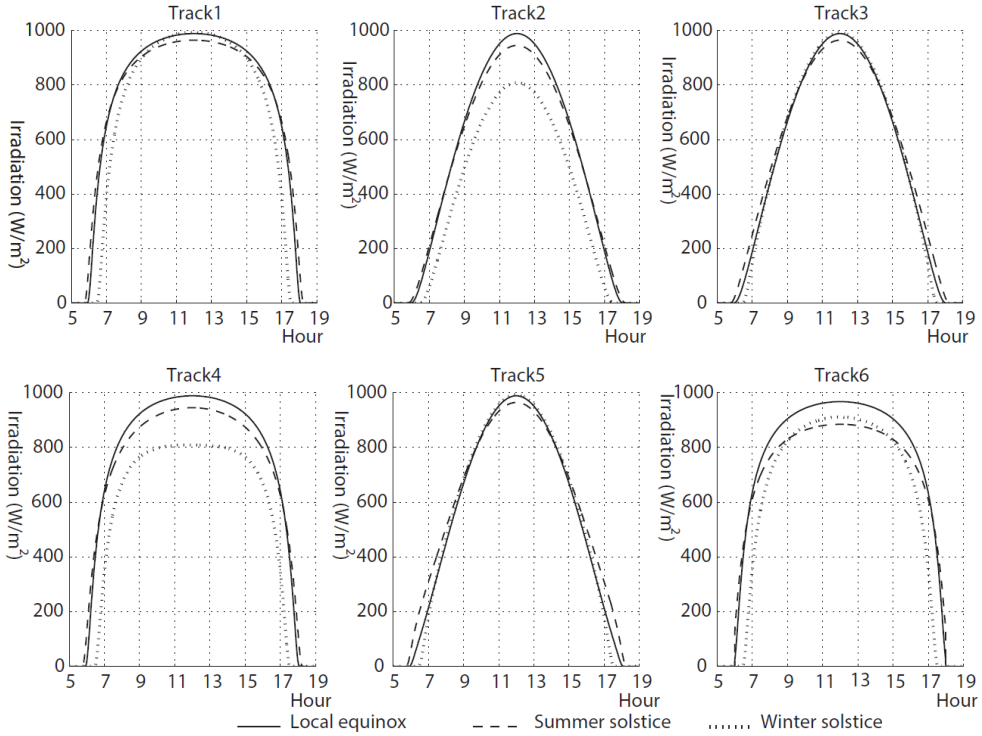

Fig. 4 Evolution of irradiation (W/m²) during clear sky according to the type of sun tracker, to the hour, and the three chosen periods.

Table 3 Daily energy collected at the collector aperture from 6:00 to 18:00.

Type of sun tracker	Daily energy (kWh/m²)			Percentage compare to **Track1** (full tracking) (%)		
	N_{jr} 112	N_{jr} 172	N_{jr} 355	N_{jr} 112	N_{jr} 172	N_{jr}355
Track1	9.77	9.76	8.78	100	100	100
Track2	7.08	6.78	5.28	72.5	69.5	60.1
Track3	7.08	7.29	7.02	72.4	74.7	80.0
Track4	9.74	9.42	7.41	99.7	96.5	84.4
Track5	7.17	7.53	7.14	73.4	77.2	81.3
Track6	9.56	8.93	8.06	97.8	91.5	91.7

The same shapes of layouts are obtained for **Track1**, **Track4** and **Track6**, with a fast increase of irradiation level, so that it exceeds $400\ W/m^2$ for winter solstice and $600\ W/m^2$ for local equinox and summer solstice after 7:00 and before 17:00. The irradiation can reach almost $800\ W/m^2$ between 9:00 & 15:00. **Track2**, **Track3** and **Track5** seem to have the same layouts curves with a slow rate of increase, so that irradiation exceeds $600\ W/m^2$ from 9:00 to 15:00. Table 3 is a comparison table which shows the energy produced from 6:00 to 18:00. It is seen that two-axis sun tracker, through **Track1** & **Track6** gives the best rate of energy 91.5% to 100%. This observation was also made by Soteris A. Kalogirou [2] for the altitude of 35 °North. Naturally, at 12 °North, the quantities of energy are quite different. For one-axis sun tracker, we notice that **Track4** leads to a rate of energy exceeding 96.5% compared to **Track1**, except during the winter solstice with 84.4%. While for the other types of sun trackers, the percentage is all day below 81.3% or 60.1% compared to Track1.

4. Conclusion

The hourly graphics established in this work, point out that all the six studied tracking approaches are suitable around 12 o'clock, showing less gap between

sun direction and concentrator's aperture normal direction, maximum irradiations level, and angular motions patterns easier to implement in an electronic card.

From 6:00 to 18:00, a two-axis sun tracker applied with **Track1** requires some precise algorithm programmation that is the major disadvantage, it makes possible to collect the maximum of energy and facilitates the use of concentrators of little acceptance angle in the transversal direction like in longitudinal direction. Over the same hours, the major advantages of **Track6** are the recurrent angular motions which shall be easier to integrate as algorithms, it allows the collecting of between 91.7% and 97.8% of energy compared to full tracking; but the required acceptance angle for the concentrator is at least 23.45 ° and 23 ° for transversal and longitudinal direction, respectively. This seems to be difficult to be reached by many conventional concentrators. The one-axis sun tracking system applied with **Track4** will give the major advantage of easier motion programmation; it makes possible the collecting of a rate of energy between 96.5% and 99.7% compared to the full tracking, except during the solstice of winter which has less than 84.4%. Another advantage is the transverse angle of incidence always near 0 °; but the major disadvantage is the longitudinal angle of incidence, which is up to 35.4 °. **Track5** shall require a hard algorithm to follow the race of the sun, it makes possible the collecting of a smaller percentage of energy between 73.4% and 81.3% compared to full tracking; its major disadvantage is the longitudinal angle of incidence which reaches 78.07 °. Fixed tracker with **Track2** and relatively fixed tracker with **Track3**, are very easy to implement, but the major disadvantage is the rate of energy collected, which is less than 74.7%; besides, the transversal and longitudinal acceptance angle need to reach 90 ° from 6:00 to 18:00.

More precisions on these results will be performed if someone transformed the used formula from earth-center frame to earth-surface frame.

References

[1] Chong, K.-K., and Wong, C.-W. 2010. "General Formula for On-Axis Sun-Tracking System." In *Solar Collectors and Panels, Theory and Applications*. London: InTech.

[2] Kalogirou, S. A. 2009. *Environmental Characteristics*. Sebastopol, CA: O'Reilly Media, Inc., pp. 49-122.

[3] ASHRAE 41.5: 1975. *Standard Measurement Guide. Engineering Analysis of Experimental Data.* ASHRAE.

[4] ANSI/ASHRAE Standard. 2007. *Ventilation for Acceptable Indoor Air Quality*. Atlanta, GA: American Society of Heat-ing, Refrigerating and Air-Conditioning Engineers, Inc.

[5] Blanco-Muriel, M., Alarcon-Padilla, D. C., Lopez-Moratalla, T., and Lara-Coira, M. 2001. "Computing the Solar Vector." *Solar Energy* 70 (5): 431-41.

[6] Grena, R. 2008. "An Algorithm for the Computation of the Solar Position." *Solar Energy* 82 (5): 462-70.

[7] Meeus, J. H. 1991. *Astronomical Algorithms*. Richmond: Willmann-Bell, Incorporated.

[8] Reda, I., and Andreas, A. 2004. "Solar Position Algorithm for Solar Radiation Applications." *Solar Energy* 76 (5): 577-89.

[9] Sproul, A. B. 2007. "Derivation of the Solar Geometric Relationships Using Vector Analysis." *Renewable Energy* 32 (7): 1187-205.

[10] Duffie, J., and Beckman, W. A. 1991. *Solar Engineering of Solar Processes*. New York: John Wiley & Sons, Inc.

[11] Kreith, F., and Kreider, J. F. 1978. *Principles of Solar Engineering*. New York: McGraw-Hill Book Company.

[12] Meinel, A., and Meinel, M. 1976. "Applied Solar Energy: An Introduction" *Physics Today* 30 (1): 66.

[13] Bernard, J. 2004. *Energie solaire: Calculs et optimisation, technosup, genie energetique*. Paris: Ellipsis Marketing, p. 383. (in French)

[14] Bernard, R., Menguy G., and Schwartz, M. 1980. "Rayonnement solaire." *Revue de géographie de Lyon* 55 (1): 92-3. (in French)

[15] Daguenet, M. 1985. *Les sechoirs solaires: theorie et pratique.* Paris: UNESCO. (in French)